Abdominal Radiology

Published online: 27 July 2018

Abdom Radiol (2019) 44:264–271
https://doi.org/10.1007/s00261-018-1712-z

Improvement of prostate cancer detection combining a computer-aided diagnostic system with TRUS-MRI targeted biopsy

Riccardo Campa,[1] Maurizio Del Monte,[1] Giovanni Barchetti,[1] Martina Pecoraro,[1] Vincenzo Salvo,[1] Isabella Ceravolo,[1] Elena Lucia Indino,[1] Antonio Ciardi,[1] Carlo Catalano,[1] and Valeria Panebianco[1]

[1]Department of Radiological Sciences, Oncology and Pathology, Sapienza University of Rome, V.le Regina Elena, 324, 00161 Rome, Italy

Abstract

Purpose: To validate a novel consensus method, called target-in-target, combining human analysis of mpMRI with automated CAD system analysis, with the aim to increasing the prostate cancer detection rate of targeted biopsies.

Methods: A cohort of 420 patients was enrolled and 253 patients were rolled out, due to exclusion criteria. 167 patients, underwent diagnostic 3T MpMRI. Two expert radiologists evaluated the exams adopting PI-RADSv2 and CAD system. When a CAD target overlapped with a radiologic one, we performed the biopsy in the overlapping area which we defined as target-in-target. Targeted TRUS-MRI fusion biopsy was performed in 63 patients with a total of 212 targets. The MRI data of all targets were quantitatively analyzed, and diagnostic findings were compared to pathologist's biopsy reports.

Results: CAD system diagnostic performance exhibited sensitivity and specificity scores of 55.2% and 74.1% [AUC = 0.63 (0.54 ÷ 0.71)] , respectively. Human readers achieved an AUC value, in ROC analysis, of 0.71 (0.63 ÷ 0.79). The target-in-target method provided a detection rate per targeted biopsy core of 81.8 % vs. a detection rate per targeted biopsy core of 68.6 % for pure PI-RADS based on target definitions. The higher per-core detection rate of the target-in-target approach was achieved irrespective of the presence of technical flaws and artifacts.

Conclusions: A novel consensus method combining human reader evaluation with automated CAD system analysis of mpMRI to define prostate biopsy targets was shown to improve the detection rate per biopsy core of TRUS-MRI fusion biopsies. Results suggest that the combination of CAD system analysis and human reader evaluation is a winning strategy to improve targeted biopsy efficiency.

Key words: Prostate cancer—Multiparametric MRI—TRUS/MRI fusion biopsy—Interventional radiology—Prostate biopsy—Computer-aided diagnosis

Prostate cancer (PCa) is the most common noncutaneous cancer in men worldwide, and the most common cancer in elderly males (> 70 years of age) in Europe [1, 2]. In their lifetime, 1/6 men will be eventually diagnosed with prostate cancer, increasing its prevalence with advancing age [3].

The European Association of Urology (EAU) guidelines advocate digital rectal examination (DRE) and PSA level measurement as first line investigation for PCa diagnosis, with TRUS-guided biopsy being the study of choice for histopathologic confirmation [2].

Recently, EAU guidelines introduced multiparametric magnetic resonance imaging (mpMRI) in the diagnostic workup of PCa due to its negative predictive value (NPV) of 86.2%–98.6% for clinically significant cancers (csPCa) (GS ≥ 7 and tumor volume > 0.5 mL, and/or extra-prostatic extension) [4, 5] and positive predictive value (PPV) of 52%–96% [6, 7]. In our highly experienced center, a recent study proved mpMRI NPV to be slightly higher than 95% for csPCa [8].

The PROMIS study assessed that the use of mpMRI can reduce the number of negative TRUS-guided random biopsies improving, nevertheless, the detection

Correspondence to: Valeria Panebianco; *email:* valeria.panebianco@gmail.com

accuracy of clinically significant prostate cancer [9]. Indeed, the specificity and sensitivity of TRUS-guided random biopsy are low for PCa detection, with a cancer detection rate (CDR) ranging from 18% to 35% [2, 10].

The exponentially growing use of mpMRI led also to an improvement of biopsy accuracy and CDR. Accordingly, MRI-targeted biopsy has been introduced in EAU guidelines as the study of choice when clinical suspicion of PCa persists despite negative biopsies, with a level of recommendation 2b [2]. The combination of mpMRI with TRUS-targeted biopsy has demonstrated a significant increase in CDR compared with standard biopsy (64% vs. 18–35%) [10–13], notably increasing the sensitivity in identifying clinically significant PCa and decreasing overdiagnosis of clinically nonsignificant PCa (GS $<$ 7) [14]. Recently, the PRECISION study group proved that the risk assessment with MRI before biopsy and MRI-targeted biopsy was superior to standard TRUS-guided biopsy in naive men at clinical risk of prostate cancer [15].

In this context, computer-aided diagnosis (CAD) systems, working by means of computer algorithms, have become one of the major research topics in medical imaging and diagnostic radiology. Different studies published in the literature have demonstrated how CAD software, incorporating different MR imaging techniques, including T2WI, DWI, and DCE [16], may help less-experienced radiologists to distinguish between benign and malignant prostate gland diseases [16–18]. The software evaluated in this study focuses its analysis on the entire prostate gland with no predilection for a specific area.

Aim of the study

The purpose of this study was to validate a novel consensus method, called target-in-target (TiT), combining human analysis of mpMRI with automated CAD system analysis (WATSON Elementary), in order to increase prostate cancer detection rate of TRUS-MRI targeted biopsy.

Materials and methods

Patient population and study design

We considered as eligible, to participate in this prospective study, all consecutive patients older than 18 yo and with high clinical suspicion for PCa (total PSA $>$ 4 ng/mL, or $>$ 2.5 in patients with family history, and/or a positive DRE) [19]. Instead, exclusion criteria were a total PSA value $>$ 20 ng/mL, previous PCa diagnosis and treatment, any contraindication to mpMRI and to transrectal prostate biopsy, urinary infection in the previous month, and alterations in patients' coagulation patterns (International Normalized Ratio, INR $>$ 1.2).

A cohort of 420 patients was enrolled, from October 2016 to June 2017, with a waiver of written informed consent. We excluded 253 patients who were not eligible to participate in this study due to the exclusion criteria previously mentioned. A total of 167 patients, aged 47–79 years, with a mean PSA value of 7.62 ng/mL (IQR 2.45–18.6), underwent diagnostic mpMRI.

All mpMRIs were analyzed by two expert urogenital radiologists and were reported, as in our current clinical practice. In addition, the same images were processed by the CAD software that brought out its own analysis and reports. Each finding has been contoured as region of interest (ROI) to extract ADC and pharmacokinetic parameters from every finding, identified by both radiologists and from CAD software.

Patients were directed to undergo biopsy when a PI-RADS score $>$ 3 was reported; however, among patients who had a reported PI-RADS score equal to 3 (as the highest), only those with a PSA density $\geq$ 0.15 were considered eligible to biopsy [19]. Thereafter, CAD targets were biopsied in all patients, applying some selection criteria that will be specified in the appropriate section (see below). When a CAD target overlapped with a radiologic one, we performed the biopsy in the overlapping area which we defined as TiT. A total of 71 patients were referred to biopsy; however, 8 patients refused to participate to this step of the study (the majority chose different centers and were lost for further follow-up during the process). Finally, we performed TRUS-MRI fusion biopsy in 63 patients, with a total of 221 sampled targets (Table 1 and Fig. 1).

MpMRI acquisition protocol

All exams were carried out with a 3.0 Tesla (Discovery 750 GE, Italy) mpMRI, using a 32 multichannel surface phased-array body coil (TORSOPA) at the Department of Radiology, "Policlinico Umberto I" of Rome.

The exams were performed with a multiparametric approach. Specifically, multiparametric MRI harvest functional information in addition to the conventional morphologic information (T2W), by correlating T2WI to diffusion (DWI) and perfusion (DCE) studies. The morphologic images were obtained using Fast Recovery Fast Spin Echo (FRFSE) T2WI on axial and coronal planes (RT: 4500 ms; ET: 120 ms; Average: 4; Slice Thickness: 3 mm; Matrix: 352 $\times$ 352; FOV: 22 cm; Scan Time: 3.30 min) with parameters' optimization, yielding a high spatial resolution. DCE studies were obtained by LAVA Gradient-Echo sequences T1W (RT: 4.5 s; ET: 1.5 s; flip angle: 15°; Average: 4; Slice Thickness: 2 mm; Matrix: 320 $\times$ 320; FOV: 22 cm; Scan Time: 3.13 min) using a body-weight adjusted intravenous bolus of contrast media (Gadovist, 0.1 mmol/Kg) (Table 2). Mean acquisition time was 17 min. A dedicated software for viewing and analysis of intensity-time curves was applied

Table 1. Patients and lesions characteristics

	Patients population and targets characteristics	
	Men included in the study, *n*	167
	Age, mean (IQR)	62 (46–78)
	Pre-biopsy PSA level, ng/mL, mean	7.62 ng/mL
RAD	PI-RADS < 3 lesions on mpMRI, *n*	30
	PI-RADS = 3 lesions on mpMRI, *n*	86
	PI-RADS = 4 lesions on mpMRI, *n*	74
	PI-RADS = 5 lesions on mpMRI, *n*	34
	Lesions identified in AS, *n*	40
	Lesions identified in PZ, *n*	166
	Lesions identified in TZ, *n*	18
CAD	MAI < 0.6 target on CAD evaluation, *n*	54
	MAI 0.6–0.69 targets on CAD evaluation, *n*	78
	MAI 0.7–0.79 targets on CAD evaluation, *n*	36
	MAI ≥ 0.8 targets on CAD evaluation, *n*	10
	Lesions identified in AS, *n*	33
	Lesions identified in PZ, *n*	60
	Lesions identified in TZ, *n*	125
Biopsy	Patients undergoing to fusion biopsy, *n*	63
	Total number of targets, *n*	221
	MpMRI targets' biopsied, *n*	118
	CAD targets' biopsied, *n*	81
	Target into target lesions' biopsy, *n*	22
	MpMRI targets' positive biopsy, *n*	81
	CAD targets' positive biopsy, *n*	29
	Target-in-target lesions' positive biopsy, *n*	18
Pathology	GS 6 (3 + 3), *n*	45
	GS 7 (3 + 4), *n*	10
	GS 7 (4 + 3), *n*	46
	GS ≥ 8, *n*	27

MpMRI, multiparametric MRI; IQR, interquartile range; PSA, prostate-specific antigen; GS, Gleason score; RAD, radiologist's evaluation; MAI, malignancy attention index; CAD, computer-aided diagnosis; AS, anterior fibromuscular stroma; PZ, peripheral zone; TZ, transition zone

Biopsy cores were considered positive when a Gleason Score equal or higher than 3 + 3 was reported

to DCE images (Olea Sphere v2.2). DWI studies were performed using Echo Planar Imaging (EPI) with multiple diffusion gradient values (*b* value 0–50–150–200–250–800–1500 s/mm^2) increasing the difference among water molecules diffusion in the extracellular space to differentiate pathologic tissues from disease-free tissues. Multiple *b* values are required for CAD system analysis to acquire and analyze images, preventing bias. ADC maps were computed from DWI by means of a dedicated software (GE Healthcare workstation).

Images analysis

Two urogenital radiologists with 10 and 15 years of prostate imaging experience, blindly evaluated all exams adopting PI-RADSv2 scoring system (RAD) [14, 20] and the CAD software (Watson Elementary, Watson Medical, Den Ham, The Netherlands).

Interreader agreement was excellent ($k = 0.918$); there were only four cases in which there was some disagreement between readers. Differences in opinion were resolved by consensus, assuming the most experienced reader's opinion as the definitive one.

Radiologist evaluation (RAD)

MpMRI images were evaluated and reported using PI-RADS v2 score system [14]. Radiologists contoured the region of interest (ROI) of all PI-RADS score ≥ 3 lesions in order to define targets for biopsy and to extract ADC and pharmacokinetic parameters from all of them.

CAD analysis (CAD)

The CAD system we evaluated (Watson Elementary) is a workflow-based viewing and trend-display tool that employs an algorithm to compute a voxel-per-voxel expectation value for neoplastic transformations, based on the combined analysis of T2W, DWI, and DCE images. This so-called Malignancy Attention Index (MAI) ranges in value from 0 to 1, with 0 and 1 indicating the lowest and the highest expected levels of neoplastic transformation, respectively. The MAI colorimetric map can be overlaid on the T2W images to easily correlate MAI with prostate morphology showing low values in blue and high values in red. Taking a cue from previous studies [21] and from manufacturer's instructions, we identified as CAD targets each highlighted area with a MAI > 0.6 and a volume > 0.1 cc; we contoured each one in order to define targets for biopsy and to extract ADC and pharmacokinetic parameters.

CAD analysis takes on average 10 min including the MAI map computation and the contouring of all suspected areas.

CAD analysis boundary conditions

As part of our analysis of the stand-alone diagnostic performance of the CAD system, we distinguished situations in which all technical boundary conditions were met from those in which one or more of the boundary conditions were potentially not met. The second situation was representative for the assessment of the overall effect of the TiT method on per-core detection rate, in order to verify it in a clinical practice scenario and not in a technical research one.

We will now provide a summary of the most important technical conditions to be fulfilled and the consequences of not fulfilling them.

DCE:

- To successfully capture and analyze the shape of the DCE curves, a minimum time resolution of 1 image volume acquisition per 10 s is needed.
- A minimum number of 4 nonenhanced image volumes must be acquired to establish a reliable pedestal value.
- A period of at least 1 min, following the enhancement peak should be observed to establish a reliable washout slope. In practice, because the time of occurrence of the enhancement peak cannot be predicted, a

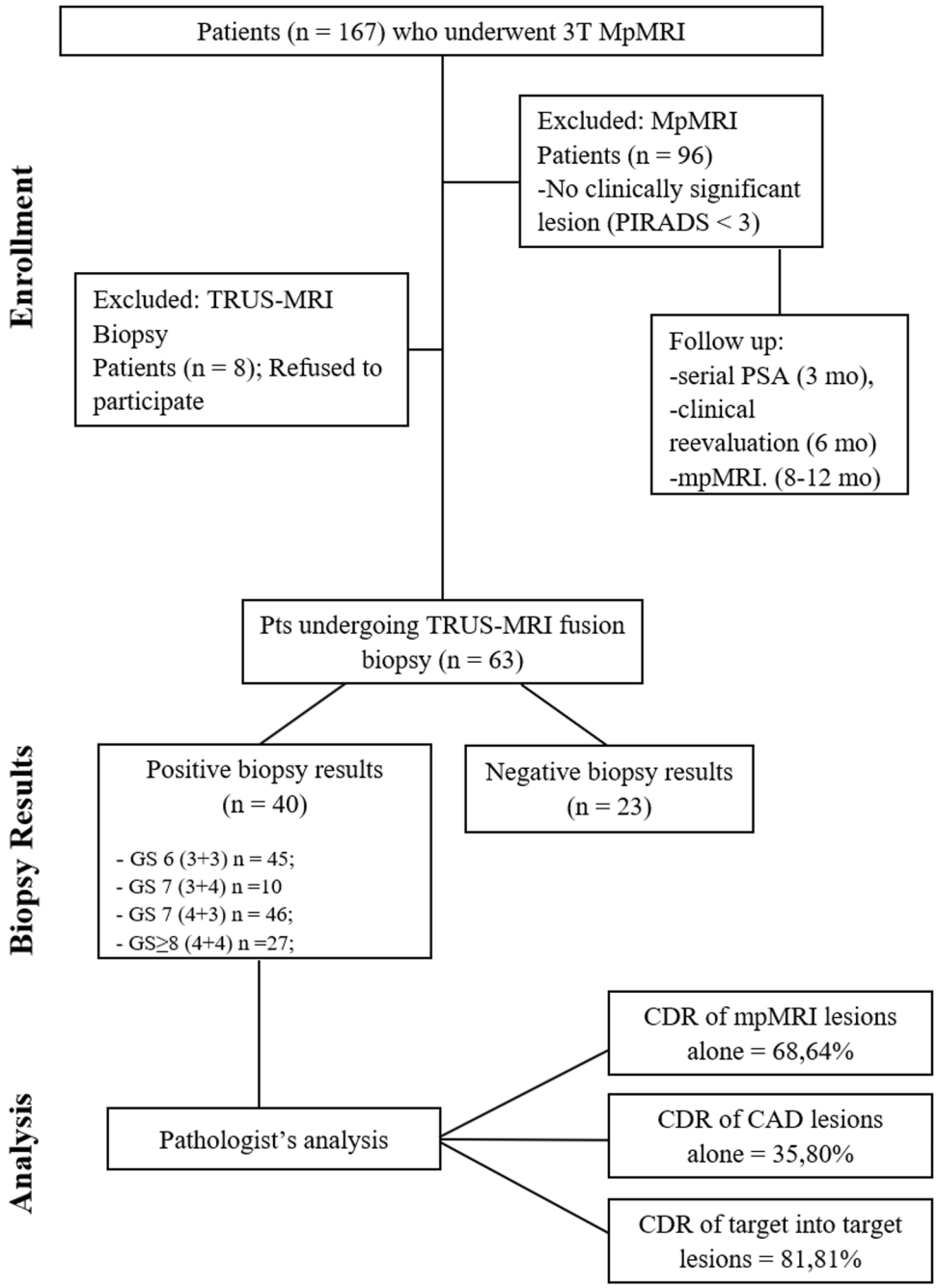

Fig. 1. Flowchart describing the design of the study.

longer time is taken. Therefore, a minimum total observation period of 3 min is recommended.
– Prostate motion should be reduced as much as possible.
– The femoral arteries must be inside the field of view.

DWI:

– Susceptibility artifacts, for instance, due to gas in the patient's rectum, or the presence of artificial hip joint elements, will adversely influence the reliability of quantitative assessment, at least in those areas where the artifacts are present.

MRI/TRUS fusion-targeted biopsy

Before the procedure, antiplatelet therapy was interrupted within 5 days (after consultation with the general practitioner and/or the specialist) and blood tests (performed within 2 weeks) including blood count, erythrocyte sedimentation rate (ESR), coagulation test (PT and

Table 2. MRI detailed parameters for T2WI and T1WI on a clinical 3T scanner

Sequence type	Gradient echo	Spin echo
Acquisition plane	Axial	Axial and coronal
RT (s)	4.5	4.5
TE (s)	1.5	1.2
Number of averages	4	4
Slice thickness (mm)	2	3
Matrix	320 × 320	352 × 352
Scan time (minutes)	3.13	3.30
FOV (cm)	22	22

RT, repetition time; ET, echo time; FOV, field of view

PTT), total PSA, and free PSA were evaluated. Prophylactic fluoroquinolones antibiotic administration was initiated 3 days before the procedure and continued for 2–3 days thereafter. Medication for bowel movement and for rectal cleaning was administered on the morning of the procedure. No local anesthesia was offered except for the administration of endorectal Lidocaine gel (10 mL), and patients were monitored for at least 60 min after the procedure.

We defined as biopsy targets all the suspicious areas identified by radiologists (RAD) and by CAD system (CAD); furthermore, we delineate as target-in-target the overlapping areas between RAD and CAD targets (Fig. 2). Targeted biopsy was performed using a transrectal approach using a dedicated system (UROSTATION KOELIS). During the procedure, an 18-gage fully automated needle is inserted and attached to the US probe; the operator acquires a virtual biopsy image with the software taking into account the needle orientation. Next, the real biopsy is performed, and a 3D-US acquisition is done with the needle inserted as well. In our protocol, the maximum number of targets to sample was three, both for radiologist and CAD evaluation, and the number of biopsy sample per lesion ranged from 2 to 4 to obtain specimen of adequate length and integrity. When the number of targets exceeded thee, priority was given to the RAD targets with a PI-RADS > 3 and subsequently to the CAD targets with a MAI > 0.7, in order not to exclude a biopsy target whit a PI-RADS 4 or 5 under any circumstances.

Once the biopsy cores were sampled and stored in formalin boxes, they were reported with a standardized

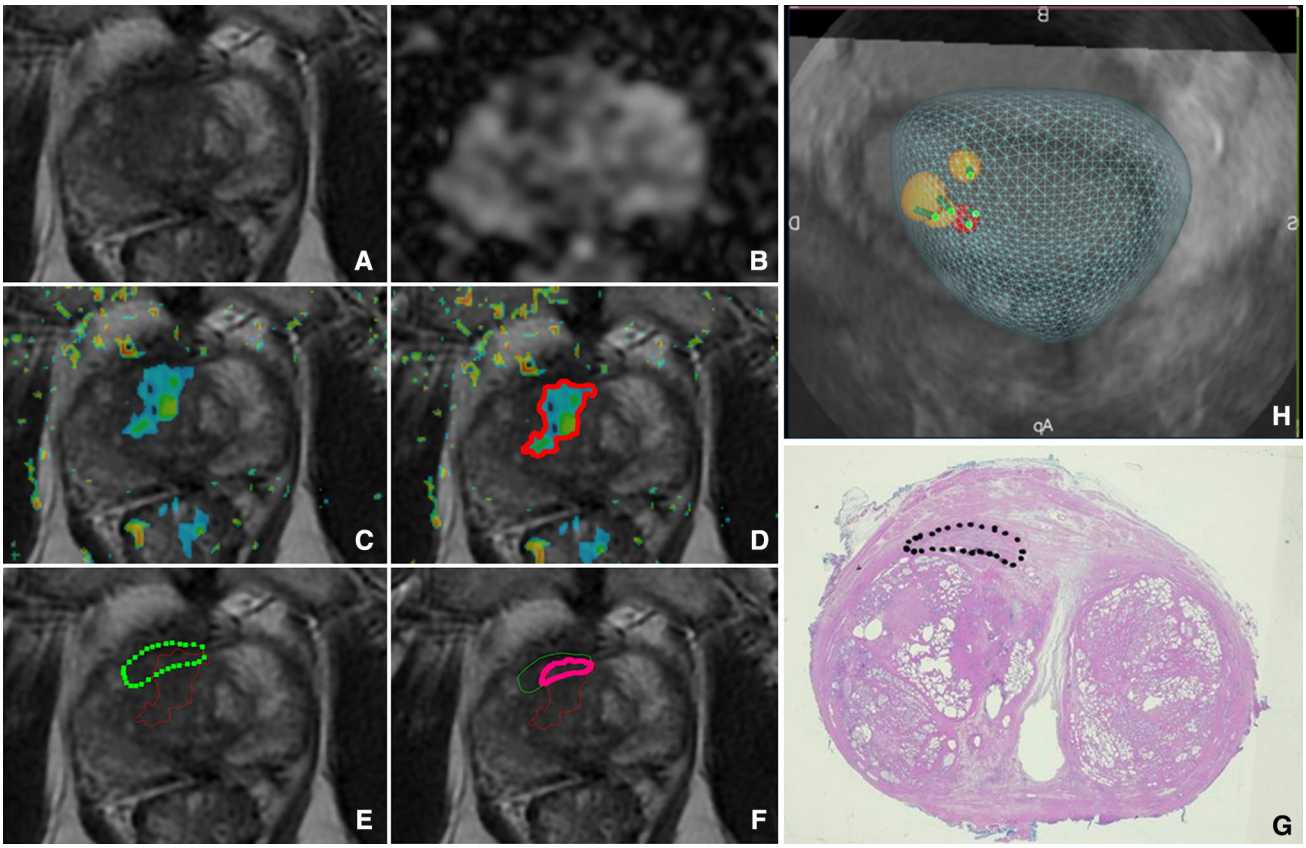

Fig. 2. Patient with suspect mpMRI finding in the mid-right anterior stroma of the gland, classified by pathologist analysis as Gleason Score 7 (3 + 4). **A** Axial T2WI; **B** ADC map; **C** MAI color map overlapped to T2WI; **D** CAD target contoured in red; **E** RAD target contoured in green; **F** Target-in-target contoured in pink; **G** 3D prostate reconstruction made by the UROSTATION KOELIS software during the TRUS-MRI fusion biopsy showing the needle traces; **H** Radical prostatectomy macrosection with the GS7 area contoured in black.

nomenclature, in concordance with the 39-sector map of the prostate from PI-RADS v2 [14], in order to avoid bias during the pathology analysis, which was performed by a pathologist with a minimum of 10-year experience in prostate analysis. In order to compare the CDR of the different targets, we considered as output, the percentage of cancer per biopsy core reported by the pathologist.

Statistical analysis

To evaluate the diagnostic performance of the CAD system, receiver operating characteristics (ROC) curves were computed for both the radiologist evaluation and the CAD analysis, using TRUS-MRI fusion-targeted biopsy as the reference test for histopathology confirmation. We used Wilcoxon-signed-rank test for the hypothesis test. We considered a $P \leq 0.05$ as statistically significant. Youden's J statistic was made to select the best MAI cutoff value. Targets' ADC and k trans values were acquired to quantitatively analyze the difference between RAD and CAD analyses. Furthermore, we compared the different detection rates (in terms of positive percentage cores) obtained from radiologist and CAD targets, using as output only the histopathologic results of TRUS-MRI fusion biopsy performed in our center.

Statistical analysis was performed using IBM SPSS Statistics v23.

Results

Biopsy cores and patients were considered positive when a Gleason Score equal or higher than 3 + 3 was reported. We considered as negative patients the 95% of those who did not show an increasing risk of prostate cancer by clinical, laboratory, or by imaging (DRE, PSA, mpMRI) in the 8-month follow-up after a negative mpMRI or a negative MRI-TRUS fusion biopsy, as suggested by the literature [10, 15, 22, 23].

The TiT method, used to combine human reader analysis with automated CAD analysis, provided a detection rate per targeted biopsy core of 81.8 % vs. a detection rate per targeted biopsy core of 68.6 % for pure PI-RADS based target definitions. Although there are no statistically significant differences with respect to the number of csPCa due to the small sample in the study, in 78% of patients with a TiT, the samples obtained from the latter possessed the highest Gleason Score reported in the patient. Only in one case, TiT sample was negative and another target (specifically a RAD target) was positive (non-csPCa). These findings give an idea of the low false-negative rate (1/18) of the TiT method even in case of a small patient sample.

The stand-alone diagnostic performance of radiologists was assessed by generating a ROC curve, varying PI-RADS score. Applying Youden J statistics, optimal values for sensitivity and specificity were found to be 56.7% and 81.5%, respectively, at a minimum PI-RADS score of 3 (i.e., PI-RADS ≥ 3). The Area Under the Curve (AUC) was 0.72 (95% CI 0.63–0.79).

We established optimal values for the MAI cutoff value in both situations, as well as sensitivity and specificity values in these optimal points (Youden's index). The optimal MAI cutoff value for positive readings was 0.55, with the resulting sensitivity and specificity values of 72.2% and 75%, respectively.

Manufacturers stated that CAD boundary conditions were fully met in 53% of cases. In 38% of cases, there were missing acquisitions at critical points in time in DCE sequences. In 10% of cases, there were susceptibility artifacts influencing DWI-based calculations/reading. In 10% of cases, there was more than 5 mm of prostate motion at critical points in time or a permanent shift. We analyzed results achieved regardless of CAD technical boundary conditions, in order to simulate more properly a clinical practice scenario, which, even while using cutting-edge technologies and all the necessary precautions, will always include the presence of some artifacts or minimal technical errors.

Therefore, the diagnostic performance of the CAD system was lower than the RAD one, AUC in this case was 0.63 (95% CI $0.54 \div 0.71$) (Fig. 3). The per-core detection rate in CAD-indicated lesions was 35.8%. Wilcoxon-signed-rank test proved the appropriateness of the analysis ($P < 0.0001$) (Table 3). ADC mean values of RAD and CAD targets did not differ much (73.25 vs. 62.4×10^{-9} mm^2/s), instead k trans values did, k trans

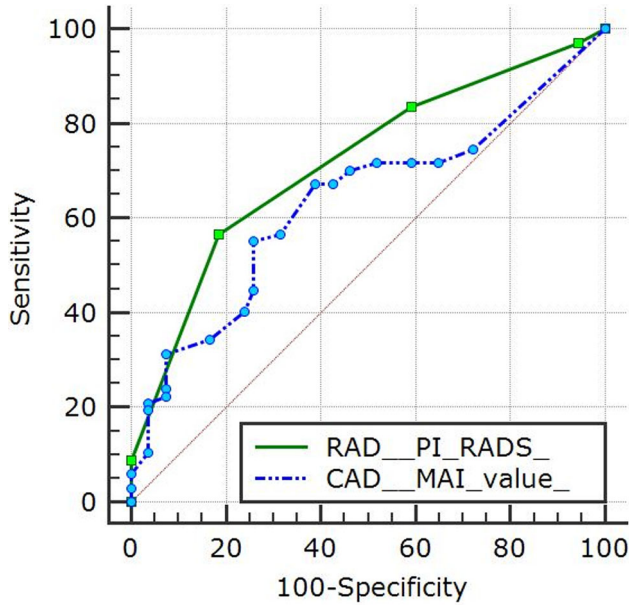

Fig. 3. ROC curve showing the comparison of RAD and CAD stand-alone diagnostic performances. Both curves reject the null hypothesis. We used 0.1 cc as volume cutoff for both CAD and RAD findings.

Table 3. Wilcoxon test (paired samples) applied to CAD and RAD diagnostic data

Wilcoxon test (paired samples)	
Large sample test statistic Z	9.545861
Two-tailed probability	$P < 0.0001$

CAD, computer-aided diagnosis; RAD, radiologist' evaluation

Table 4. ADC and *k* trans values plotted on the table for both the RAD and CAD evaluations

	ADC			*k* trans		
	Mean	SD	CI 95%	Mean	SD	CI 95%
PI-RADS ≥ 3	73.25	23.17	69.59–76.90	0.35	0.43	0.24–0.35
MAI ≥ 0.6	62.46	15.76	59.87–65.06	0.59	0.21	0.51–0.66

k trans values are higher in CAD
ADC, apparent diffusion coefficient; CAD, computer-aided diagnosis; RAD, radiologist' evaluation; SD, standard deviation; CI, confidence interval; MAI, malignancy attention coefficient

was higher in CAD (0.35 vs. 0.59 min^{-1}) (Table 4). The overall PCa detection rate was 60.4%.

Discussion

The results of this study suggest that a well-defined consensus method, combining automated CAD analysis of mpMRI with PI-RADS based analysis performed by human readers is a promising way to improve the per-core detection rate of targeted biopsies. Several interesting discussion points also arise from the study results.

We would like to address the differences in diagnostic performance of the different components combined in the consensus method, being the stand-alone performance of the CAD system and the stand-alone performance of human readers.

The most striking performance difference found in the overall results is that human readers showed a markedly higher per-core detection rate than the CAD system (68.6% vs. 35.8%). However, through the consensus approach, the overall per-core detection rate was significantly improved (from 68.6% to 81.8%). The results showed that in 78% of patients, TiT samples possessed the highest Gleason Score reported in the patient, which increases the safety that a patient has a csPCa or not, potentially reducing the cases in which a patient inserted in an active surveillance protocol is ruled out by a following biopsy that confirms a Gleason Score higher than the first one.

The study results show that human readers are less influenced by technical imaging flaws and artifacts than the CAD system. This effect expresses itself as a better detection specificity for human readers, at almost equal sensitivity, which is indicative of the CAD system generating a higher number of false-positive readings when analyzing data that falls outside its defined ideal operating envelope, thus reducing its per-core detection efficiency. However, the overlapping of RAD- and CAD-indicated areas constitutes a meaningful selection mechanism to define relevant areas.

From a more detailed analysis of the results, it followed also that the CAD system in some cases seems to overestimate the likelihood of PCa by assigning higher significance to DCE parameters. ADC mean values of radiologic and CAD targets did not differ much, instead *k* trans values did, being higher in CAD targets. Especially in the transition zone of the prostate, this represents a well-known potential cause of false-positive readings.

In conclusion, the improved per-core detection rate, provided by the TiT consensus method appears to be the result of counteracting the flaws of the individual reading methods.

The study results show that adhering to the CAD system's technical boundary conditions appears to be a major factor influencing the quality of the system's diagnostic capabilities. Human readers were less influenced by imaging flaws and artifacts. This suggests that results could be further improved by increased quality control, focused on the needs of CAD systems. Thus far, with human readers being less influenced by technical artifacts, this need may have been present to a less extent.

Given the results of the TiT method for lesions with PI-RADS score 3 and higher, an intriguing question for further research arises—whether this method can be used to assign patients with a PI-RADS score 3, yet with a negative TiT score—to an MRI-based follow-up protocol, rather than to biopsy. The suggestion would be to perform a 6–8-month imaging follow-up. However, more research of the CAD software NPV would be needed before implementing such a regime.

Limitations of the study

Our study is subject to limitations. First, when calculating CDR, our investigation focused on biopsy results obtained only in our center bypassing those obtained by other operators with possible different methods. Second, when assessing the diagnostic AUC curve performance, we have considered also biopsy results obtained by other centers, with different working teams (operators, pathologist, etc.) and even if the approaches are standardized, this might have caused possible bias. Third, data from whole-mount reports are required to precisely correlate MAI values with histopathology.

There are concerns about the men with negative results on multiparametric MRI who do not undergo biopsy. It has been shown that these men have a low risk of clinically significant cancer, but nonetheless, follow-up with monitoring of the PSA level is routine, reasonable, and safe [15]. In addition, several studies proved that

previous well-designed studies have highlighted that the percentage of cases of clinically significant cancer that are missed by MRI-targeted biopsy but detected by standard transrectal ultrasonography–guided biopsy is low, between 0% and 10% [10, 22, 23].

Conclusion

We believe that the value of the CAD system is best exploited by deploying it in conjunction with human reader assessment. We demonstrated how employing this approach, the per-core detection rate in TRUS-MRI-targeted biopsies can be significantly increased.

Furthermore, future studies are believed valuable to investigating into the role of the CAD system for PI-RADS 3 lesions decision making. We suggest investigating a potential regime in which patients with ''target-in-target'' PI-RADS 3 lesions could be candidates for targeted biopsy. Instead, patients with PI-RADS 3 lesions with negative CAD results could undergo clinical follow-up at 6–8 months. In such an investigation, long-term follow-up would be required to properly evaluate the negative predictive value of CAD software for PCa detection in PI-RADS 3 findings.

Compliance with ethical standards

Funding No funding was received for this research.

Conflict of interest All the authors declare that they have no conflict of interest.

Ethical approval All procedures performed in studies involving human participants were in accordance with the institutional board and the ethical standards of the institutional and national research committee and with the 1964 Helsinki declaration and its later amendments or comparable ethical standards.

Informed consent Informed consent was obtained from all individual participants included in the study.

References

1. De Angelis R, et al. (2014) Cancer survival in Europe 1999–2007 by country and age: results of EUROCARE-5—A population-based study. Lancet Oncol 15(1):23–34
2. Mottet N, et al. (2017) EAU-ESTRO-SIOG guidelines on prostate cancer. Part 1: screening, diagnosis, and local treatment with curative intent. Eur Urol. 71(4):618–629
3. Cancer Facts & Figures (2017). American Cancer Society.
4. Itatani R, et al. (2014) Negative predictive value of multiparametric MRI for prostate cancer detection: outcome of 5-year follow-up in men with negative findings on initial MRI studies. Eur J Radiol 83(10):1740–1745
5. Schimmöller L, et al. (2014) Predictive power of the ESUR scoring system for prostate cancer diagnosis verified with targeted MR-guided in-bore biopsy. Eur J Radiol 83(12):2103–2108
6. Moore CM, et al. (2013) Image-guided prostate biopsy using magnetic resonance imaging-derived targets: a systematic review. Eur Urol 63(1):125–140
7. Thompson J, Lawrentschuk N, Frydenberg M, et al. (2013) The role of magnetic resonance imaging in the diagnosis and management of prostate cancer: the role of magnetic resonance imaging in the diagnosis and management of prostate cancer. BJU Int 112:6–20
8. Panebianco V, et al. (2018) Negative multiparametric magnetic resonance imaging for prostate cancer: what's next? Eur Urol 74(1):48–54
9. Ahmed HU, et al. (2017) Diagnostic accuracy of multi-parametric MRI and TRUS biopsy in prostate cancer (PROMIS): a paired validating confirmatory study. Lancet 389(10071):815–822
10. Siddiqui MM, et al. (2015) Comparison of MR/ultrasound fusion-guided biopsy with ultrasound-guided biopsy for the diagnosis of prostate cancer. JAMA 313(4):390
11. Radtke JP, et al. (2016) Multiparametric magnetic resonance imaging (MRI) and MRI–transrectal ultrasound fusion biopsy for index tumor detection: correlation with radical prostatectomy specimen. Eur Urol 70(5):846–853
12. Filson CP, et al. (2016) Prostate cancer detection with magnetic resonance-ultrasound fusion biopsy: the role of systematic and targeted biopsies: CaP detection with MR-US fusion biopsy. Cancer 122(6):884–892
13. Salami SS, et al. (2015) In patients with a previous negative prostate biopsy and a suspicious lesion on magnetic resonance imaging, is a 12-core biopsy still necessary in addition to a targeted biopsy?: performance of mpMRI in predicting prostate cancer on repeat biopsy. BJU Int 115(4):562–570
14. Barentsz JO, et al. (2016) Synopsis of the PI-RADS v2 guidelines for multiparametric prostate magnetic resonance imaging and recommendations for use. Eur Urol 69(1):41–49
15. Kasivisvanathan V, et al. (2018) MRI-targeted or standard biopsy for prostate-cancer diagnosis. N Engl J Med. https://doi.org/10.1056/NEJMoa1801993
16. Hambrock T, Vos PC, Hulsbergen–van de Kaa CA, Barentsz JO, Huisman HJ (2013) Prostate cancer: computer-aided diagnosis with multiparametric 3-T MR imaging—Effect on observer performance. Radiology 266(2):521–530
17. Doi K (2007) Computer-aided diagnosis in medical imaging: historical review, current status and future potential. Comput Med Imaging Graph 31(4–5):198–211
18. Vos PC, Hambrock T, Barenstz JO, Huisman HJ (2010) Computer-assisted analysis of peripheral zone prostate lesions using T2-weighted and dynamic contrast enhanced T1-weighted MRI. Phys Med Biol 55(6):1719–1734
19. Epstein JI (1994) Pathologic and clinical findings to predict tumor extent of nonpalpable (Stage T1 c) prostate cancer. JAMA 271(5):368
20. Simonetti G (2010) *Imaging RM della prostata*. Milan: Springer
21. Roethke MC, et al. (2016) Evaluation of an automated analysis tool for prostate cancer prediction using multiparametric magnetic resonance imaging. PLoS ONE 11(7):e0159803
22. Panebianco V, et al. (2015) Multiparametric magnetic resonance imaging vs. standard care in men being evaluated for prostate cancer: a randomized study. Urol Oncol Semin Orig Investig 33(17):1–7
23. Wysock JS, et al. (2014) A prospective, blinded comparison of magnetic resonance (MR) imaging-ultrasound fusion and visual estimation in the performance of MR-targeted prostate biopsy: the PROFUS trial. Eur Urol 66(2):343–351